





LETTER | JULY 08 2024

## Magnetic resonance velocimetry reveals secondary flow in falling films at the microscale

Georges C. Saliba   ; Jan G. Korvink  ; Juergen J. Brandner 

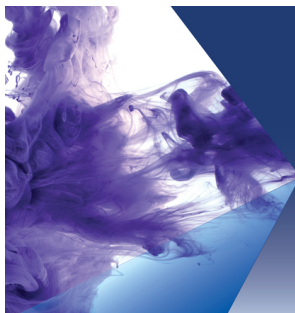


*Physics of Fluids* 36, 071705 (2024)

<https://doi.org/10.1063/5.0214609>



23 July 2024 05:06:05



## Physics of Fluids

Special Topic:

Recent Advances in Fluid Dynamics and its Applications

Guest Editors: B.Reddappa, B. Rushi Kumar, Sreedhara Rao Gunakala, Bijula Prabhakar Reddy

[Submit Today!](#)

# Magnetic resonance velocimetry reveals secondary flow in falling films at the microscale

Cite as: Phys. Fluids **36**, 071705 (2024); doi: 10.1063/5.0214609

Submitted: 18 April 2024 · Accepted: 18 June 2024 ·

Published Online: 8 July 2024



View Online



Export Citation



CrossMark

Georges C. Saliba,<sup>1,a)</sup>  Jan G. Korvink,<sup>1</sup>  and Juergen J. Brandner<sup>1,2</sup> 

## AFFILIATIONS

<sup>1</sup>Institute of Microstructure Technology (IMT), Karlsruhe Institute of Technology (KIT), Hermann-von-Helmholtz-Platz 1, 76344 Eggenstein-Leopoldshafen, Germany

<sup>2</sup>Karlsruhe Institute of Technology, Karlsruhe Nano Micro Facility KNMFi, Hermann-von-Helmholtz-Platz 1, 76344 Eggenstein-Leopoldshafen, Germany

<sup>a)</sup>Author to whom correspondence should be addressed: [georges.saliba@kit.edu](mailto:georges.saliba@kit.edu)

## ABSTRACT

To design better falling film microreactors, concrete knowledge of the flow and the ability to produce complex channel structures are necessary. The efficiency of falling film microreactors is most often determined by studying the composition of the liquid after it has exited the system. In the present study, Magnetic Resonance Velocimetry is used to obtain three-dimensional, three-component velocity fields inside of falling films flowing in open microchannels. The microchannels were made by two-photon polymerization. It was possible to resolve the complex shape of the liquid–gas interface and to observe, for the first time, secondary flow inside of a falling film at the microscale.

© 2024 Author(s). All article content, except where otherwise noted, is licensed under a Creative Commons Attribution-NonCommercial 4.0 International (CC BY-NC) license (<https://creativecommons.org/licenses/by-nc/4.0/>). <https://doi.org/10.1063/5.0214609>

There is an unmet need for more efficient gas–liquid contactors. In the case of falling film microreactors, two major hurdles have to be overcome to facilitate further advances: measuring the flow and producing complex channel structures. A deeper understanding of flow dynamics affords a rational approach to designing microreactors. Mixing rates, turbulence levels, film thickness, and velocity distribution, among other things, can serve as a guide to tailoring the flow to specific needs. This fundamental gain in knowledge can then be translated into new more complex channel geometries, made using micro-fabrication techniques. An iterative process can then take place whereby new designs are reliably tested and, in light of additional measurement results, further refined. In the realm of falling film microreactors (FFMRs), studies that look into the hydrodynamics of the system currently rely heavily on simulations.<sup>1,2</sup> As a result, experiments are only performed on simple channel geometries producing single-component velocity fields.

However, secondary flow can occur in a falling film and can be triggered by concentration gradients in the liquid phase, which lead to surface tension gradients. Sobieszuk *et al.*<sup>3</sup> showed that, in a microreactor, the absorption rate of CO<sub>2</sub> in a CO<sub>2</sub>-monoethylamine(MEA)-H<sub>2</sub>O system was four times higher than in a CO<sub>2</sub>-NaOH-H<sub>2</sub>O system. The same phenomenon occurs at larger scales and is attributed to the appearance of Marangoni cells due to surface tension inhomogeneities

that appear in the CO<sub>2</sub>-monoethylamine(MEA)-H<sub>2</sub>O system.<sup>4,5</sup> Nevertheless, Sobieszuk *et al.*<sup>3</sup> only speculated on the presence of secondary flow in their micro-falling film by drawing a comparison with large-scale flow. No direct measurements were performed to study the flow. It is worth noting that the secondary flow in this particular case depended on the reactions studied.

Another, simpler way of inducing secondary flow is by modifying the structure of the channel. At low Reynolds numbers, the flow in an open channel is laminar and mass transport from the interface across the depth of the film occurs mainly through diffusion, which is inherently a slow process. A properly mixed solution ensures an even distribution of reagents and maintains a high concentration gradient of the absorbed substance across the gas–liquid interface. In microfluidic systems, passive solutions are often sought out to improve mixing. In the context of closed-channel microfluidic mixers, where two or more miscible fluids are involved, there is a wide variety of passive designs to choose from. The review by Hessel *et al.*<sup>6</sup> presents a large number of them, based, for example, on interdigital multi-lamellae arrangements, split-and-recombine (SAR) concepts, or collision of jets. They also present a class of devices based on “chaotic mixing by eddy formation and folding.” Meandering channels belong to this category and rely on secondary flow induced by the curvature of the flow path.<sup>7,8</sup> The curvature of the channel results in centrifugal forces that shift the location of

the maximum velocity from the axis of the channel outward with respect to the center of curvature. A positive pressure gradient then arises between the outer and inner sides of the channel. The fluid at the center of the channel is then pushed outward, leading to the formation of a vortex pair. A series of alternating curved microchannels can then produce chaotic mixing. Another approach consists in adding diagonal grooves at the bottom of the channel across the streamwise direction. The fluid flow inside the groove is deviated sideways, leading to flow recirculation.<sup>7</sup>

Stroock *et al.*<sup>9</sup> patterned the bottom of the channel with staggered herringbone motifs to induce chaotic mixing in the flow. The fluid flows into these grooves, which are placed across its flow path. This, in turn, induces a transverse flow component, which then develops into circulating flow. In other words, vortex cells appear in the transverse plane that changed positions along the flow direction. The channels were patterned using planar lithography. The same pattern was also used for open channel flows in the context of falling film microreactors.<sup>2,10,11</sup> However promising, these studies relied either on flow simulations or on characterizing the solution at the outlet of the system to evaluate the performance of the microreactor.

The present work lies at the crossroads of microfabrication technology, experimental fluid mechanics, and nuclear magnetic resonance. Using two-photon polymerization to produce micro-structured channels, in conjunction with magnetic resonance velocimetry to characterize the resulting flow, enables us to pull the study of the hydrodynamics of falling film microreactors out of the numerical realm and to set it on a firm experimental footing. Two main design strategies were considered here: (1) bas-relief patterns formed at the bottom of rectangular channels and (2) channels with continuously varying depth and width. For bas-relief patterning, the same design used by Al-Rawashdeh *et al.*<sup>2</sup> was reproduced, which was originally adapted for an open channel configuration from Stroock *et al.*<sup>9</sup> In the second design, both the depth and the width of the channel have a sinusoidal shape. In the case of a pressure-driven flow inside of a closed microchannel, changing the cross section along the axial direction accelerates or decelerates the flow in the streamwise direction. For open channel microflows, and because of surface tension, if the channel becomes wider, the film stretches sideways, reducing its thickness orthogonally, while increasing the length of the interface. As a result, the expansion of the channel increases the local surface-to-volume ratio of the film. The chaotic mixer and variable cross section designs serve two different purposes. In the open channel chaotic mixer, the laminar flow is periodically folded onto itself, through the action of vortices in the transverse plane. In the channels with variable cross section, the film is periodically stretched and compressed, leading to an axially variable surface-to-volume ratio.

A common method to measure velocity using NMR is to encode the motion into the phase of the spin magnetization. In this case, spins act as magnetic moments, and as they travel through a magnetic field gradient, their precession rate experiences a related phase shift, imprinted on the phase of the magnetization. If the magnetic field gradient is linear, the phase shift gained in unit time is proportional to displacement and hence velocity along the direction of the gradient. The advantage of this technique is that it offers a direct velocity measurement from the moving fluid's nuclei, unlike hot-wire velocimetry, which is indirect, where heat rapidly spreads and where the probe can disturb the flow, or PIV/PTV, which actually measures the speed of the seeding particles and not that of the fluid itself.

Magnetic Resonance Imaging and Nuclear Magnetic Resonance Spectroscopy are closely associated with the fields of medicine and chemistry, respectively. However, the same underlying principles can be used to perform velocity measurements on systems of interest to engineers. Magnetic Resonance Velocimetry has been successfully used to study turbulent flow in a variety of engineering applications.<sup>12,13</sup>

In order to encode velocity and obtain a signal from the spins, an NMR pulse sequence must be applied. Typical pulse sequences involve a radio frequency pulse, combined with a set of timed magnetic field gradients in the  $x$ ,  $y$ , and  $z$  directions, resulting in a radio frequency echo from the sample, which is then measured and analyzed. These different elements overlap in order to perform operations such as slice selection (the position of the plane of measurement), velocity encoding, and  $k$ -space sampling for the in-plane location. More concretely, nuclei with nonzero magnetic moments subjected to a strong magnetic field  $B_0$  will start precessing at the Larmor frequency  $\omega_0$  given by

$$\omega_0 = \gamma B_0, \tag{1}$$

where  $\gamma$  is the gyromagnetic ratio, which is a characteristic of the nucleus. If a linear magnetic field gradient  $G$  [ $\text{mTm}^{-1}$ ] (which could be time-dependent, i.e.,  $G = G(t)$ ) is applied along a given direction, say  $x$ , the precession frequency will depend on the positions of the nuclei according to

$$\omega_0(x) = B_0 + G \cdot x. \tag{2}$$

The position  $x$  of a nucleus can then be expanded as

$$x(t) = x_0 + \frac{dx}{dt}t + \frac{1}{2!} \frac{d^2x}{dt^2}t^2 + \frac{1}{3!} \frac{d^3x}{dt^3}t^3 + \dots \tag{3}$$

$$= x_0 + vt + \frac{1}{2!}at^2 + \frac{1}{3!}jt^3 + \dots, \tag{4}$$

where  $v$  denotes velocity,  $a$  acceleration, and  $j$  jerk. The phase of a nucleus is then determined as the integral of  $\omega_0$  during a given time, i.e.,

$$\phi(x, t) = \gamma \int_0^t (B_0 + G(\tau) \cdot x(\tau)) d\tau, \tag{5}$$

$$= \gamma \int_0^t \left[ B_0 + G(\tau) \cdot \left( x_0 + v\tau + \frac{1}{2}a\tau^2 + \dots \right) \right] d\tau, \tag{6}$$

$$= \gamma \left[ x_0 \int_0^t G(\tau) d\tau + v \int_0^t \tau G(\tau) d\tau + \frac{1}{2}a \int_0^t \tau^2 G(\tau) d\tau + \dots \right]. \tag{7}$$

If the time-dependent gradient  $G(t)$  has a net area of zero and if we ignore the higher-order moments  $\int_0^t \tau^n G(\tau) d\tau$  for  $n > 1$ , then the following relationship between phase and velocity can be established:

$$\phi = \gamma M_1 v, \tag{8}$$

where  $M_1 = \int_0^t \tau G(\tau) d\tau$ . In other words, applying a magnetic field gradient across the sample leads to a dependence between the phase and the positions of the nuclei, which can then be used, by applying a well-designed time-dependent gradient, to create a relationship

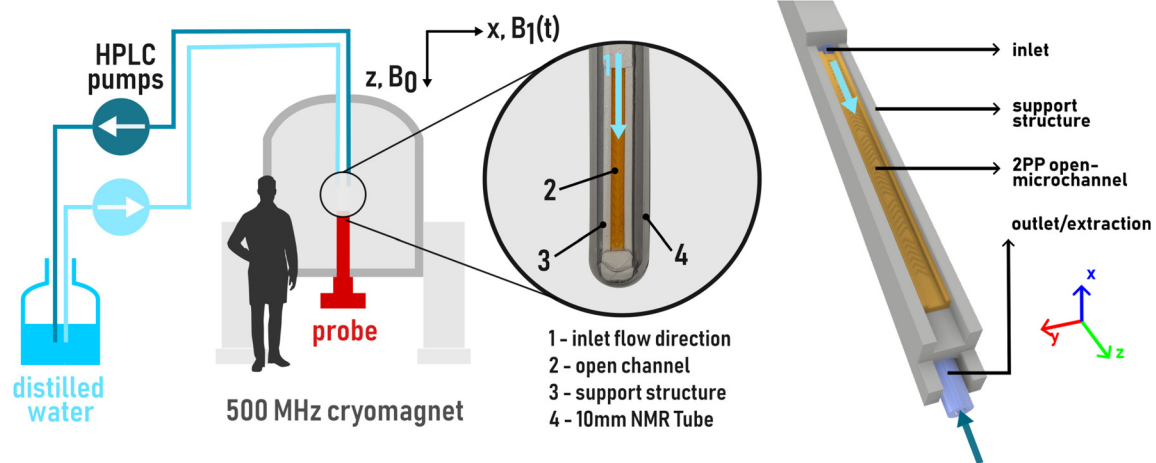


FIG. 1. Schematic diagram of the experimental setup (left) with a rendering of the open channel and the support structure (right).

between phase and velocity. What was presented so far is only an outline of the theory underlying magnetic resonance velocimetry using phase encoding. The reader is referred to specialized texts, such as Fukushima<sup>12</sup> or Elkins and Alley,<sup>13</sup> for a more extensive presentation of the topic.

In the present study, a standard Cartesian 4D MRV sequence (“FLOWMAP,” ParaVision 6.0.1, Bruker BioSpin MRI GmbH, Ettlingen, Germany) was used. The sequence was composed of a 3D gradient-echo and a 4-point Hadamard velocity encoding scheme.<sup>14</sup> The investigator interrogates the sample using an RF pulse. The spins in the sample, which are subject to a strong polarizing magnetic field, respond via an echo, which is measured by the RF coil. In the case of MR velocimetry, the response of the sample will depend on the strength of the magnetic field and how it is distributed, both of which can be controlled by using magnetic gradient coils. The amplitude and duration of the gradients can be controlled individually along the three spatial axes to encode spatial and velocity information into the spins, which can then be measured.

To our knowledge, the only other work to study falling films using MR velocimetry was reported by Heine *et al.*<sup>15</sup> Nevertheless, their work considers falling films in a channel that is 40 mm wide, whereas the open channels presented here are at most 1.4 mm. This means that the curvature of the interface is much more significant in the present case, which has an effect on the flow.

Regarding post-processing, MRV offers an additional advantage over micro-PIV, PTV, and all derived techniques, in that the velocity maps are obtained directly after the experiment is done. The measured signals undergo a Fourier transform, which results in a spatial distribution of the three components of the velocity vector. Further processing is possible in MATLAB to obtain quantities such as the surface-to-volume ratio of the film, the shear stress at the interface, and the volume flow rate. The contours of the film in each cross-sectional slice is detected by first binarizing the velocity map, with a threshold of  $V_{th} = 0.1 \text{ mms}^{-1}$ . The bwboundaries function was then used to trace the boundary of the film. Compared to micro-PIV for instance, the high computational costs required to deduce velocity fields from optical raw data are avoided. Transferring data from the MRI acquisition

software (ParaVision) to post-processing tools, such as ParaView, is a straightforward affair. The images are saved by the MRI software as 2dseq files, which can easily be read into MATLAB using code from Bruker. The three-component, three-dimensional velocity fields can then be saved as RAW files, which are compatible with the ParaView visualization software.

The experiments were performed inside of an 11.7T nuclear magnetic resonance system ( $^1\text{H}$  resonance frequency of 500 MHz, Bruker BioSpin). Radio frequency coils used in magnetic resonance spectroscopy experiments are expected to hold standard-sized test tubes filled with chemicals. For this reason, probe heads are not typically designed for flow experiments and offer limited space, which is not an issue considering the size of our system. A Micro5 MR microscopy probe with a maximum gradient of  $3 \text{ Tm}^{-1}$  was used. The probe is equipped with a 10 mm receiver/transmitter saddle coil supported on glass mounts. The inner volume of the coil was only accessible from above. A diagram of the setup is shown in Fig. 1.

The QuantumX 2PP system from NanoScribe was used to produce the micro-structured open channel. Microscope images of the printed parts are shown in Figs. 2(b) and 3(a) for the wavy and heringbone channels, respectively. All designs fit inside of a  $1 \times 2 \times 50 \text{ mm}^3$  volume. The only difference is the shape of the open channel. A holder for the channel was made out of PLA by fused filament fabrication (FFF or FDM), more commonly known as filament 3D-printing. The channel is held in place mechanically. The holder fits vertically inside of the 10 mm NMR test tube. Two identical HPLC pumps (KNAUER 40P, Berlin, Germany), with  $10 \text{ ml min}^{-1}$  pump heads and running at the same flow rate, were used to feed the channel and then extract the water that accumulates at the bottom of the tube, eliminating the need for additional sensors.

A white light microscope image of the top of the open wavy channel is presented in Fig. 2(b). The total width of the part is 2 mm and a section 7.6 mm long was imaged. Both the velocity field and the shape of the falling film can be extracted from the data and are shown in Fig. 2(c). The surface of the film exhibits a complex curvature since the film is stretched and compressed in the width direction, modifying the shape of the meniscus. As mentioned earlier, the complex

curvature of the surface constitutes a major hurdle for any optical technique since it acts as an additional lens in the pathway of the light beam, which has to be corrected. Keeping in mind that the curvature depends both on channel geometry, which we aim to optimize, and on flow rate, optically correcting the data would become an intractable task. Another solution consists in matching the refractive index of the liquid to that of the channel, then placing the camera on the other side of the flow, i.e., on the side of the channel. However, this limits the choice of liquid that can be used.

From the perspective of microreactor development, this design results in a nonuniform surface-to-volume ratio because the film is periodically thinned out and then compressed. The surface-to-volume ratio  $S_v$  along a single motif of the wavy pattern is plotted in Fig. 2(d). Within this interval, the value of  $S_v$  fluctuates between around  $3000$  and  $6000\text{m}^2\text{m}^{-3}$ . The distance between the two side-walls of the channel varies periodically between  $1$  and  $1.4$  mm. The advantage of this design is that the film is thinned out only for a short distance (and hence time) along the flow before being compressed again, which prevents the appearance of dry patches, which can develop for low flow rates and wide channels.

The open channel with the herringbone bas-relief design is shown in Fig. 3(a). It was produced using the same technology as for the wavy channel, and it has a similar maximum extent of  $1 \times 2 \times 50\text{mm}^3$ . Unlike the flow in the wavy channel, the liquid-gas interface in this configuration is patently unaffected by the presence of grooves at the bottom of the channel. This is clearly reflected both in the shape of the interface, shown in Fig. 3(b), and the surface-to-volume ratio, Fig. 3(c), which fluctuates with a relative standard deviation of less than 5%. However, what is interesting in this channel design is that it induces secondary flow. In order to show the secondary flow, streamlines were plotted with the inlet plane as the starting point. A streamwise projection of these streamlines is shown in Fig. 4 for two different flow rates. A pair of counter-rotating vortices can be discerned in the transverse plane. Their relative sizes and positions are determined by the herringbone pattern.<sup>9</sup> In closed-channel microfluidic systems, this design is used to rapidly mix two liquids. In the present configuration, it serves to transport the absorbed gas away from the surface of the film. This convective mass transport is much more efficient than diffusion, to remove the mixture from the contact surface, and contributes to

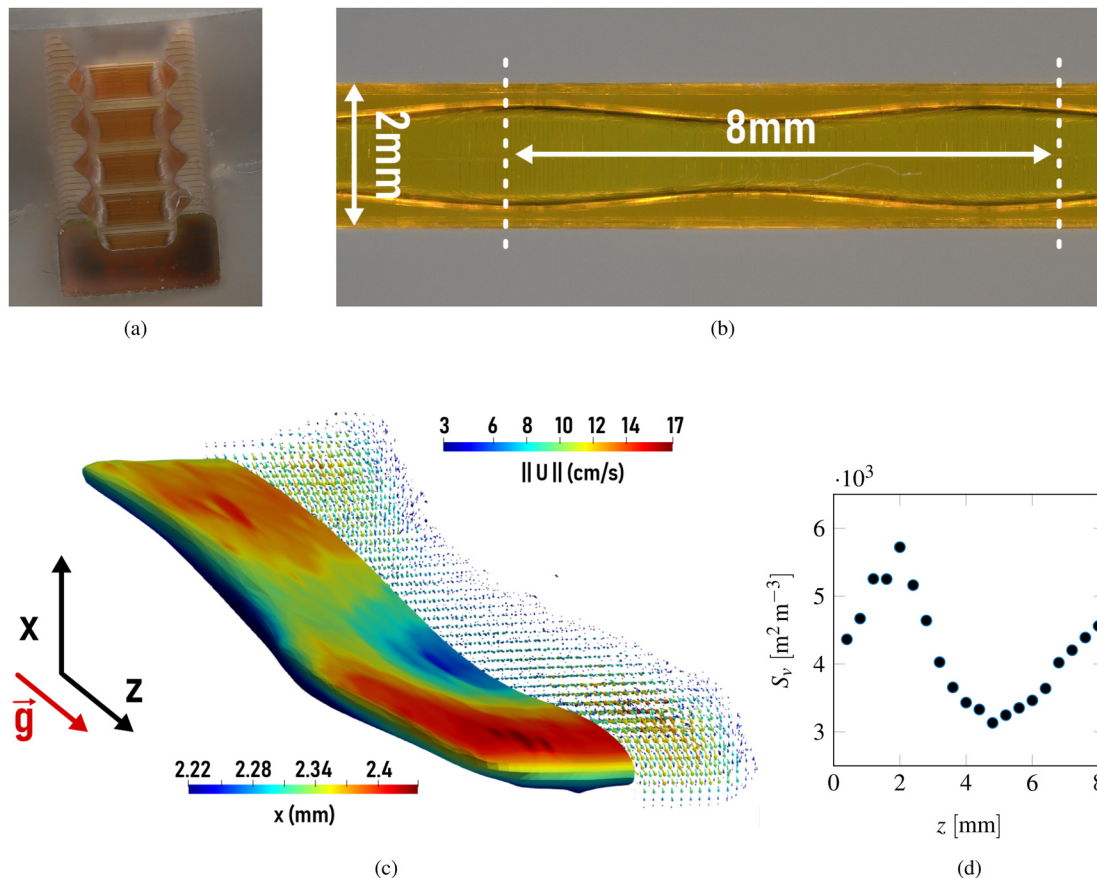


**FIG. 2.** Flow measurements inside of the “wavy” channel. (a) Tilted and (b) top views of the open channel geometry with variable width and depth made by two-photon polymerization. The deepest point coincides with the narrowest channel width and vice versa. (c) The flow is measured experimentally within a window that is 8 mm long in the  $z$ -direction. On the left, the surface of the film is colored according to height relative to an arbitrary reference, and on the right, the vector field is indicated, with color representing velocity. Gravity acts along the  $z$  axis. (d) The surface-to-volume ratio  $S_v$  of the film at different  $z$ -positions, from geometry data measured. The surface-to-volume ratio fluctuates between  $3000$  and  $6000\text{m}^2\text{m}^{-3}$  with an average value of  $4200\text{m}^2\text{m}^{-3}$ . The volumetric flow rate was  $1\text{ml min}^{-1}$ .



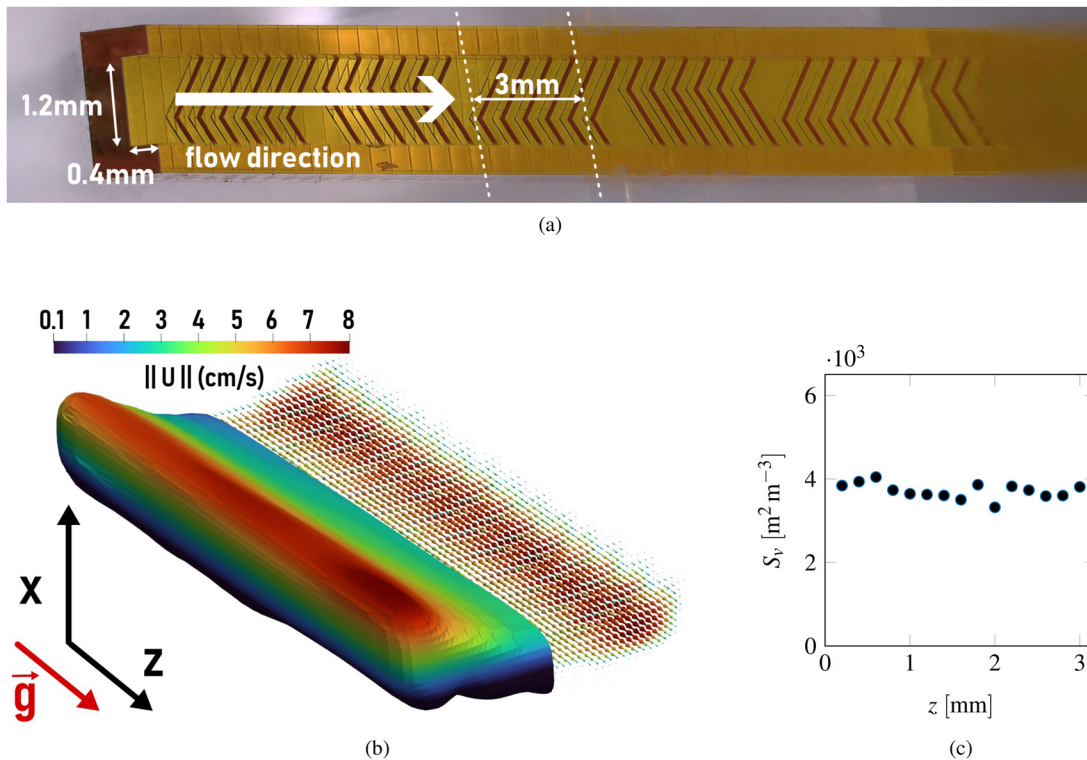


**FIG. 3.** Experimental results from the herringbone channel. (a) Micromanufactured channel showing the repeated herringbone geometry. (b) The surface of the film (left cut, colored according to  $x$ -position), and the three-component, three-dimensional velocity field (right cut). Gravity acts along the  $z$  axis. (c) The surface-to-volume ratio along the channel. Unlike the flow in the wavy channel, the surface of the film here is undisturbed by the presence of the bas-relief patterns. This is reflected in the surface-to-volume ratio, which remains stable at  $3709\text{m}^2\text{m}^{-3}$ , with a relative standard deviation of less than 5%. The volumetric flow rate was  $1\text{ml min}^{-1}$ .

maintaining a high concentration gradient across the interface and hence a high gas absorption rate.

In summary, magnetic resonance velocimetry is a modern and powerful flow measurement technique suited for studying falling films in microreactors. Two different design principles for falling film microreactors were investigated, with the aim of controlling absorption and

mixing of a gas phase in a liquid film at the microscale. The complex open channels were made by two-photon polymerization. In the first case, the shape of the open channel led to an intricate topology of the gas-liquid interface, as well as a periodic thinning of the film with a lower risk of breakup or dry-patch formation. Using MRV, it was possible for the first time to measure the flow inside an open microchannel

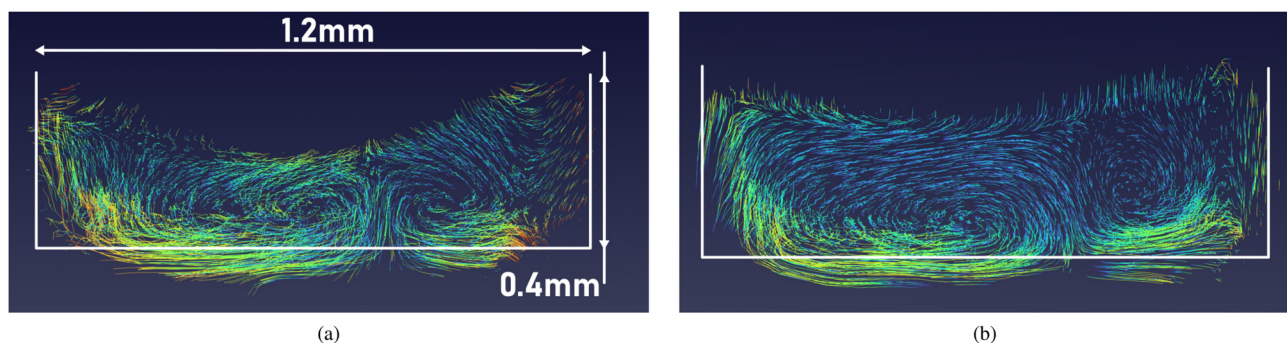


**FIG. 4.** View of the streamlines along the film, in the flow direction. The color indicates the integration time along each streamline. Both figures correspond to channels that are  $400\ \mu\text{m}$  and  $1200\ \mu\text{m}$  wide with herringbone patterns  $200\ \mu\text{m}$  deep. The left figure shows a film flow at  $1\text{ml min}^{-1}$  and the right at  $2\text{ml min}^{-1}$ . As known from closed-channel herringbone micromixers, two counter-rotating vortices appear, the right vortex rotating in the clockwise direction. The white line corresponds to the inner contour of the channel, the streamlines below it corresponds to flow in the channels of the bas-relief pattern.

with a chaotic mixer design. Aside from the novelty of the results, this experimental method affords information that is difficult to obtain directly, or even inaccessible, for most other measurement techniques, especially optical ones such as PTV and micro-PIV. To date, studies on falling film microreactors have either relied on simulating the system, or the liquid was experimentally characterized only at the outlet of the system.<sup>1,2</sup> The present study, however, outlines a process by which one can produce complex channel structures, characterize the flow itself, and then reiterate. It becomes possible to rationalize the design of a microreactor by setting it on firm experimental grounds.

G.C.S. and J.G.K. acknowledge partial funding through the ERC Synergy Grant No. 951459 (HiSCORE). JJB and JGK acknowledge support from the DFG for funding the CRC 1527 (HyPERiON). JJB and GCS acknowledge partial support of the Karlsruhe Nano Micro Facility (KNMF), a Helmholtz Research Infrastructure at the Karlsruhe Institute of Technology.

## AUTHOR DECLARATIONS

### Conflict of Interest

The authors have no conflicts to disclose.

### Author Contributions

**Georges Saliba:** Conceptualization (equal); Formal analysis (lead); Investigation (lead); Methodology (lead); Visualization (lead); Writing – original draft (lead). **Jan Gerrit Korvink:** Conceptualization (equal); Funding acquisition (equal); Project administration (equal); Supervision (equal); Writing – review & editing (equal). **Juergen Brandner:** Conceptualization (equal); Funding acquisition (equal); Supervision (equal); Writing – review & editing (equal).

### DATA AVAILABILITY

The data that support the findings of this study are available from the corresponding author upon reasonable request.

## REFERENCES

- <sup>1</sup>N. Steinfeldt and N. Kockmann, “Experimental and numerical characterization of transport phenomena in a falling film microreactor with gas-liquid reaction,” *Ind. Eng. Chem. Res.* **59**, 4033–4047 (2020).
- <sup>2</sup>M. Al-Rawashdeh, A. Cantu-Perez, D. Ziegenbalg, P. Löb, A. Gavriilidis, V. Hessel, and F. Schönfeld, “Microstructure-based intensification of a falling film microreactor through optimal film setting with realistic profiles and in-channel induced mixing,” *Chem. Eng. J.* **179**, 318–329 (2012).
- <sup>3</sup>P. Sobieszuk, R. Pohorecki, P. Cygański, M. Kraut, and F. Olschewski, “Marangoni effect in a falling film microreactor,” *Chem. Eng. J.* **164**, 10–15 (2010).
- <sup>4</sup>K. Warmuziński, J. Buzek, and J. Podkański, “Marangoni instability during absorption accompanied by chemical reaction,” *Chem. Eng. J. Biochem. Eng. J.* **58**, 151–160 (1995).
- <sup>5</sup>J. Buzek, J. Podkański, and K. Warmuziński, “The enhancement of the rate of absorption of CO<sub>2</sub> in amine solutions due to the Marangoni effect,” *Energy Convers. Manage.* **38**, S69–S74 (1997).
- <sup>6</sup>V. Hessel, H. Löwe, and F. Schönfeld, “Micromixers-A review on passive and active mixing principles,” *Chem. Eng. Sci.* **60**, 2479–2501 (2005).
- <sup>7</sup>F. Schönfeld and S. Hardt, “Simulation of helical flows in microchannels,” *AIChE J.* **50**, 771–778 (2004).
- <sup>8</sup>F. Jiang, K. S. Drese, S. Hardt, M. Küpper, and F. Schönfeld, “Helical flows and chaotic mixing in curved micro channels,” *AIChE J.* **50**, 2297–2305 (2004).
- <sup>9</sup>A. D. Stroock, S. K. W. Dertinger, A. Ajdari, I. Mezic, H. A. Stone, and G. M. Whitesides, “Chaotic mixer for microchannels,” *Science* **295**, 647–651 (2002).
- <sup>10</sup>M. Al-Rawashdeh, V. Hessel, P. Löb, K. Mevissen, and F. Schönfeld, “Pseudo 3-D simulation of a falling film microreactor based on realistic channel and film profiles,” *Chem. Eng. Sci.* **63**, 5149–5159 (2008).
- <sup>11</sup>D. Ziegenbalg, P. Löb, M. Al-Rawashdeh, D. Kralisch, V. Hessel, and F. Schönfeld, “Use of ‘smart interfaces’ to improve the liquid-sided mass transport in a falling film microreactor,” *Chem. Eng. Sci.* **65**, 3557–3566 (2010).
- <sup>12</sup>E. Fukushima, “Nuclear magnetic resonance as a tool to study flow,” *Annu. Rev. Fluid Mech.* **31**, 95–123 (1999).
- <sup>13</sup>C. J. Elkins and M. T. Alley, “Magnetic resonance velocimetry: Applications of magnetic resonance imaging in the measurement of fluid motion,” *Exp. Fluids* **43**, 823–858 (2007).
- <sup>14</sup>C. L. Dumoulin, S. P. Souza, R. D. Darrow, N. J. Pelc, W. J. Adams, and S. A. Ash, “Simultaneous acquisition of phase-contrast angiograms and stationary-tissue images with Hadamard encoding of flow-induced phase shifts,” *Magn. Reson. Imaging* **1**, 399–404 (1991).
- <sup>15</sup>C. Heine, K. Kupferschläger, S. Stapf, and B. Blümich, “NMR velocimetry of falling liquid films,” *J. Magn. Reson.* **154**, 311–316 (2002).